30 August 1974, Volume 185, Number 4153 SCIENCE

Tunable Laser Fluorescence Method for Product State Analysis

Laser-induced fluorescence is used as a detector of collisionally unrelaxed products of chemical reactions.

Richard N. Zare and Paul J. Dagdigian

One ultimate goal of the physical chemist who studies gas-phase reactions is the determination of "microscopic" rate constants for elementary reaction steps, such as the exchange reaction $A + BC \rightarrow AB + C$. By microscopic rate constants we mean the state-to-state constants that specify how the translational and internal quantum states of the reagents A and BC evolve into the translational and internal quantum states of the products AB and C. Philosophically, such information represents the total of all accessible information about the scattering system according to quantum mechanics, and all less-detailed measurements may be regarded as suitable averages over various microscopic rate constants. Naturally, one might begin by inquiring whether this goal has ever been achieved for any reaction system. The answer is simply no! Then, one might ask if *all* these state-to-state rate constants must be determined in order to arrive at a chemist's understanding of the reaction dynamics. The answer is, hopefully, certainly not, but, until we have the means of determining detailed rate constants, we will not be able to make generalizations with confidence.

By comparison with the information available 20 years ago, we are now fortunate indeed. This increase in understanding has been brought about largely by advances in experimental techniques, which have permitted us to abandon traditional kinetic studies in "bulbs" in favor of "beams." In bulb experiments many collisions occur between the time of reagent mixing and the time of product sampling, and the reacting volume is the entire volume of the bulb including the walls. In crossed-beam experiments chemical reactions are studied one collision at a time with an effective time resolution of about 10^{-13} second, which is the duration of a typical reactive encounter. This is accomplished by confining the reaction zone to the intersection of two beams of reactants in a chamber sufficiently evacuated so that collisions do not disrupt the straight-line motion of the reactants as the two beams approach and that of the products as they recoil from the reaction zone at some scattering angle.

From "Bulbs" to "Beams"

The relatively small number of product molecules involved in beam experiments as compared with bulb experiments places a premium on the development of sensitive detection methods. For reactive scattering experiments, it is essential to use detection systems that are extremely sensitive to the small flux of product molecules present and that are extremely specific to the identities of the reaction products so that the products can be distinguished from the overwhelmingly preponderate background of elastically scattered reactants and residual gas molecules. Table 1 summarizes the various types of molecular beam detectors employed in the past (*1*). Most involve surface effects and require a knowledge of the probability that the molecule does not bounce off the surface (sticking coefficient) if quantitative measurements are to be made. With the exception of the first two techniques in Table 1, which are of historical interest, these detection schemes can be very sensitive. Bolometers, densitometers, and scintillation counters are limited in application to special classes of atoms and molecules. Most of the detection schemes in Table 1 are not differential; that is, they do not permit differentiation between reactants and products. It is for this reason that molecular beam experiments, for example, the Stern-Gerlach experiment, the measurement of the anomalous magnetic moment of the electron, the Lamb shift, and other experiments, were until recently almost exclusively within the province of physicists rather than chemists.

Within the last two decades, surface ionization and electron bombardment ionization detectors (see Figs. 1 and 2) have opened the way to the use of molecular beams in the study of chemical reactions because with these detectors it is possible to distinguish reaction products (*2*, *3*). Recently spectroscopic techniques have also been employed to detect reaction products in beam experiments. We first discuss the application of hot-wire detectors and mass spectrometers to the study of chemical reactions and in particular to the determination of internal energy distributions. We then discuss how molecular spectroscopy may be applied to the direct determination of the internal states of the reaction products, and we conclude by describing a new technique based on the excitation of the fluorescence of reaction products by tunable lasers.

Dr. Zare is professor of chemistry at Columbia University, New York 10027. Dr. Dagdigian is a postdoctoral research associate at Columbia University and in September 1974 he will join the faculty at Johns Hopkins University, Baltimore, Maryland 21218, as assistant professor of chemistry.

Angular Distribution Studies

Molecular beam angular distribution studies excel in the elucidation of the structure and lifetime of the fleeting complex of interlocking reactants. In addition, scattering experiments allow determination of the translational energy distribution of reaction products. Figure 3 illustrates the type of information about the geometry and lifetime of the "collision complex" obtainable from angular distribution studies. Before collision, reagents of masses M_1 and M_2 approach with a relative velocity $\mathbf{v}_{rel}$ at an impact parameter b (Fig. 3A). They form a collision complex (Fig. 3B) in which the magnitude of the total angular momentum L_i equals $\mu v_{rel} b$, where $\mu = M_1 M_2/(M_1 + M_2)$ is the reduced mass. If the collision complex is long-lived, the product angular distribution measurements promode of breakup of the collision complex and not on that of its formation. The angular distribution will be symmetric about a plane perpendicular to $\mathbf{v}_{rel}$ [in the center-of-mass (CM) system] if the lifetime of the collision complex exceeds the rotational period of the collision complex. Hence, angular distribution measurements provide information on the duration of the collision complex. In addition, the geometry of a long-lived collision complex is reflected in the form of spatial anisotropy of the products (*4*). If the collision complex is oblate (pie-shaped, see Fig. 3C), the angular distribution peaks at 90° with respect to $\mathbf{v}_{rel}$ (see Fig. 3E); if it is prolate (cigar-shaped, see Fig. 3D), the angular distribution peaks forward and backward along $\mathbf{v}_{rel}$ (see Fig. 3F). On the other hand, for collision complexes that are short-lived, the angular distribution shows forward-backward asymmetry characteristic of the forces acting during the reactive encounter.

Since the experiments are performed in a laboratory frame of reference, where the CM is not at rest, the proper interpretation of the angular distribution data requires a transformation from the laboratory to the CM frame. Usually thermal (Maxwell-Boltzmann) beams are employed so that a complex convolution over beam velocities is required. In addition, the transformation depends on the velocity distribution of the products. With the introduction of velocity selectors (*5*), it is possible to simplify greatly this analysis by velocity selection of reagents or

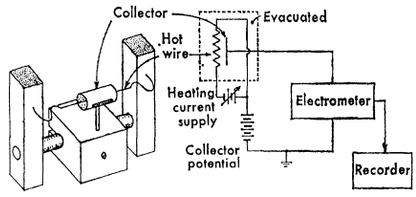

Fig. 1. Schematic diagram and view of a hot-wire detector. [Adapted from Zorn and English (*1*)]

products, or both, but with a concomitant loss in intensity.

Velocity selection allows the product recoil energy distribution to be determined. This knowledge combined with the reaction exothermicity permits one to infer how the energy of reaction is partitioned between translational and internal degrees of freedom of the products. Thus, angular distribution studies furnish indirect information on product state distributions, but only qualitative statements, such as the average internal excitation of the products, can be made. Exceptions to this generalization are those special reactions involving hydride products where the variation in the internal state quantum number of the product causes large changes in the product translational energy. A notable example is the reaction $F + D_2 \rightarrow DF + D$, which has been investigated in the elegant experiments of Schafer, Siska, Parson, Tully, Wong, and Lee (*6*). Because of the large vibrational spacing of the DF product, they were able to identify different features in their CM intensity contour map as corresponding to different DF vibrational states.

Deflection and Resonance Studies

Although neither the hot-wire detector nor the electron bombardment ionizer is sensitive to the internal state of the products (*7*), one may use external fields to gain information directly on the product internal state distribution by measuring the variation of the deflection pattern with internal state. This technique is particularly well suited for the determination of rotational distributions of polar molecules. The Stark effect depends strongly on the magnitude (J value) and orientation (M_J value) of the rotational angular momentum vector because of the different averaged torques exerted by the external field on the permanent dipole moments of molecules in the (J,M_J) state. The first application of this technique was the electric deflection studies of alkali halide products in 1965 by Herm and Herschbach (*8*), who were able to determine the average rotational energy of the products. Grice, Mosch, Safron, and Toennies (*9*) have also applied electric deflection techniques, using an electric quadrupole lens to measure the rotational energy distribution of RbBr in the reaction $Rb + Br_2$. They found that the distribution can be fitted to a Boltzmann distribution with a rotational temperature T_{rot} of 2500° ± 300°K. Electric deflection studies appear to be limited to the rotational analysis of highly polar products. Moreover, the determination of the relative populations of internal states requires a knowledge of the transmission as a function of product internal state (vibrational dependence of the dipole moment) and velocity. These corrections can be very difficult to ascertain so that this technique is best suited to the measurement of the average rotational excitation.

Electric deflection techniques can also yield information on the orientation of reaction products. Recently Maltz, Weinstein, and Herschbach (*10*), using an electric two-pole field, have found that the rotational angular momentum vector **J** of CsBr from the reaction Cs + HBr lies preferentially in a plane at right angles to the initial relative velocity vector $\mathbf{v}_{rel}$. The experimental method involves comparing deflection profiles measured with the field oriented parallel and perpendicular to the plane of the reactant beams. Maltz *et al.* have shown that the difference between these profiles depends primarily on $\langle \cos^2 \chi \rangle$, where χ is the angle between **J** and $\mathbf{v}_{rel}$.

Perhaps the ultimate molecular beam "trip" is the study of $Cs + SF_6 \rightarrow CsF + SF_5$ in 1971 by Freund, Fisk, Herschbach, and Klemperer (*11*), who "mated" a crossed-beam source with a Rabi-type molecular beam electric resonance apparatus. Using the radio-frequency (rf) spectrum of CsF, they were able to determine the relative vibrational populations in the five lowest vibrational levels for several low rotational states ($J = 1$ to 4). These experiments were repeated in an improved fashion using a supersonic Cs source by Bennewitz, Haerten, and Müller (*12*), who were able to observe $v = 0$ to 8. The vibrational energy distribution of the CsF is a Boltzmann distribution characterized by a

temperature. These results, combined with the velocity and angular distribution studies of Riley and Herschbach (*13*) and the electric deflection studies of Maltz (*14*), show that the Cs + SF_6 reaction proceeds through a long-lived collision complex in which the available energy is partitioned equally among all degrees of freedom. This reaction is probably the best-studied example of a long-lived complex. The same technique has also been applied to the reactions Cs + SF_4 (*12*) and Li + SF_6 (*15*). However, the use of a crossed-beam source with an electric resonance spectrometer is limited to reactions with large cross sections in which at least one of the products is a highly polar molecule whose rf spectrum is not complicated by large hyperfine interactions. Because only the lowest J levels can be refocused in the resonance spectrometer, the vibrational populations obtained may not be characteristic, in general, of the vibrational distribution.

Infrared and Visible Chemiluminescence

Traditionally, the most direct method for determining the internal state distributions of molecules has been optical studies carried out in absorption and in emission. Molecular spectroscopy is well suited for the determination of the identity of the reaction products because the molecular absorption or emission lines "fingerprint" the upper and lower energy level patterns; moreover, the intensities may be directly related to concentrations so that information is obtained about internal state distributions (*16*). Spectroscopic techniques find wide application in kinetic studies, such as in shock tubes, flames, discharges, flash photolyses, and flowing afterglows (*17*). A straightforward application of absorption spectroscopy to the detection of beams is not feasible because of the extremely low densities of the beam species. It appears possible to gain a factor of 100 or more in sensitivity by carrying out intracavity absorption, in which the absorbers are placed inside the cavity of a laser. Although this technique (*18*) has recently been used to detect trace chemicals and free radicals, its application to beams has not been demonstrated. It is not surprising then that optical spectroscopy has played almost no role in the de-

Table 1. Traditional molecular beam detectors of neutral species.

Physical or chemical process	Detector
Condensation of beam on target	Analytical balance
Pressure of beam on target	Pirani gauge
Chemical attack of target by beam	Densitometer
Recombination of condensed beam on target	Bolometer
Radioactivity of condensed beam on target	Scintillation counter
Ejection of electrons from target by beam of metastables	Auger detector
Surface ionization of beam on target	Hot-wire detector
Electron bombardment ionization of beam	Mass spectrometer

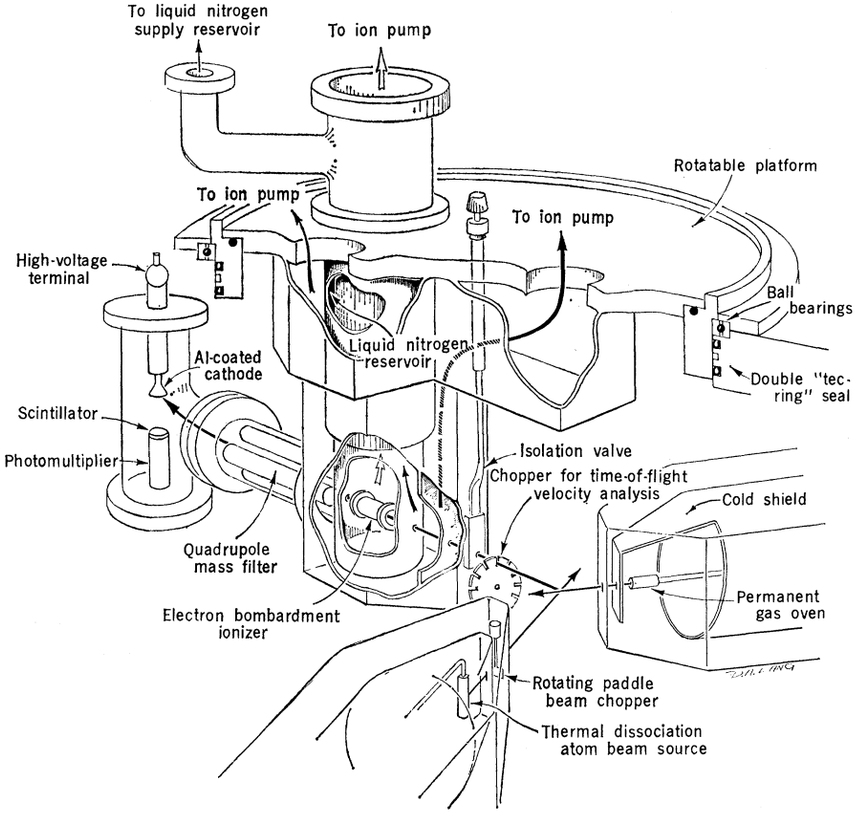

Fig. 2. Cutaway view of a molecular beam scattering apparatus with a mass spectrometer detector. [From McDonald *et al.* (*55*); courtesy of the American Institute of Physics, New York]

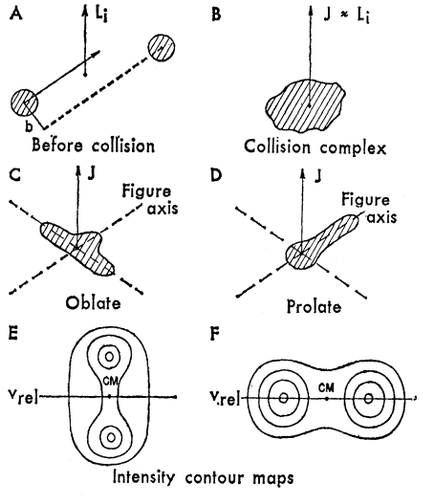

Fig. 3. Schematic representation of the information obtainable from molecular beam angular distribution studies. In (A), the reactants approach one another with relative velocity v_{rel}. The impact parameter b is defined as the distance of closest approach, if there were no interaction between the reactants (straight-line trajectories). When the reactants come together, they form a collision complex (B), which in some reactions has a lifetime for breakup longer than the rotational period. The geometry of the "collision complex" is then reflected in the shape of the angular distribution: The CM angular distributions will be of the form in (E) or in (F) if the collision complex is oblate (C) or prolate (D), respectively. [Adapted from a slide of A. Henglein]

velopment of beam technology (*1*), although the absorption of resonance radiation has been used to deflect atomic beams (*19*).

In contrast to absorption spectroscopy, emission studies hold promise of being much more sensitive since the signal of interest is not obscured by a large background at the same wavelength. In particular, vibrationally excited reaction products may emit an infrared photon in undergoing the vibration-rotation transition $(v',J') \rightarrow (v'',J'')$. Beginning with the pioneering work of Cashion and Polanyi (*20*), infrared chemiluminescence has been applied to the study of the kinetics of chemical reactions, and this technique has provided thus far, perhaps, the richest source of information on the internal state distributions of reaction products. Because infrared lifetimes are typically 10^{-3} second or longer, early studies suffered from collisional degradation of the initial energy distribution. However, Polanyi and his co-workers (*21*) have been able to approach collision-free conditions by their "arrested flow" technique, in which the products are removed rapidly by cryopumping. In this manner, they have been able to obtain rotational as well as vibrational population distributions of the freshly formed products. This technique showed for the first time that the rotational distributions vary from one vibrational level to another. Using a low-pressure flow apparatus, Jonathan and his co-workers (*22*) and others have measured vibrational populations, but no information on the rotational distributions could be obtained because of the rapid collisional thermalization of this degree of freedom.

Infrared chemiluminescence has been almost exclusively limited to studies involving the hydrogen halides. These molecules have been chosen because their radiative lifetimes are especially short, their collisional relaxation rates are particularly slow, and their infrared spectra fall in the region from 2 to 4 microns where infrared detectors are most sensitive. As a result of recent technical advances, such as improved detectors, Fourier transform techniques, and the ability to remove blackbody background radiation by cooling both the vacuum chamber and the spectrometer to 85°K or less, McDonald and his co-workers (*23*) have observed the chemiluminescence of reaction products in the 10-micron region, where many organic molecules fluoresce.

The signal-to-noise problems inherent in the detection of infrared chemiluminescence may be overcome if the reaction products are used as the active medium for an infrared chemical laser (*24*). However, because chemical lasers are operated most conveniently at pressures on the order of 10 torr or more, information about the initial rotational distribution cannot be obtained. Moreover, laser amplification can provide information only on vibrational levels showing sufficient population inversion to have measurable gain.

Visible chemiluminescence offers an alternative to infrared emission when the reaction is sufficiently exothermic that excited electronic states are produced. Because electronic lifetimes are typically on the order of 10^{-6} second or less, collisional degradation of the initial internal state distribution in visible chemiluminescence is much less important at similar pressures than in infrared chemiluminescence. For example, at pressures as high as 10^{-4} torr, on the average, the excited state radiates before suffering any collisions (single-collision conditions). Moreover, all excited products will radiate in the field of view of the detector because of their short radiative lifetimes; furthermore, detectors in the visible portion of the spectrum are superior to their infrared counterparts. Consequently, visible chemiluminescence studies, when applicable, offer a much more sensitive means of detection so that chemiluminescence can actually be observed under single-collision conditions. It must be stressed, however, that both techniques are "blind" to certain types of reaction products. Products in the $v = 0$ vibrational level cannot be detected by infrared chemiluminescence. Visible chemiluminescence studies detect only electronically excited products; consequently, information about "invisible" reactions, such as the formation of vibrationally excited ground-state products, can only be inferred. This limitation on visible chemiluminescence is particularly severe since in almost all known highly exothermic reactions the production of electronically excited products is a minor process.

The first spectroscopic studies of visible chemiluminescence of molecular species formed under single-collision conditions were carried out in 1970 by Ottinger and Zare (*25*), who studied reactions of group II A metals with various oxidizer gases. For the chemiluminescent reaction $Ba + NO_2$, it was possible to obtain rotational and vibrational population distributions of the excited BaO product as well as information on the spatial alignment of the molecules from observation of the polarization of the emission (*26*). This visible chemiluminescence technique has been applied to the study of many other highly exothermic chemical reactions, such as $Al + O_3$ (*27*). In addition, chemiluminescence studies under single-collision conditions have provided evidence on the intriguing four-center reactions $M_2 + X_2 \rightarrow MX + MX^*$, where M and X are alkali and halogen atoms, respectively (*28*). Although visible chemiluminescence is a specialized means of detecting reaction products, nonetheless this technique shows the power of visible light as a probe of the internal state distribution.

Laser-Induced Fluorescence

With the development of tunable organic dye lasers (*29, 30*) it has become possible to study with visible light "invisible reactions" in which only ground-state products are formed. Resonance fluorescence is employed to detect the reaction products. A tunable narrow-band light source is swept in wavelength. Whenever it coincides with a molecular absorption line, the reaction products make a transition to an excited electronic state from which they subsequently emit (fluoresce). This emission is detected by a photomultiplier which "views" the excitation zone. The fluorescence intensity is recorded as a function of laser wavelength to produce what we call an excitation spectrum; the intensities are then converted to relative populations of the various product internal states, with the help of vibrational and rotational intensity factors. The fluorescence is not spectrally resolved (which would require some loss of signal intensity). Instead, the narrow bandwidth of the laser provides the spectral resolution.

It might be asked whether a laser is necessary for fluorescence detection of reaction products. The following simple calculations indicate that this technique could not have been applied prior to the development of tunable lasers: Presently available pulsed dye lasers are capable of producing an

average spectral irradiance of 0.2 watt per square centimeter per angstrom, whereas intense white-light sources, such as a 1000-watt xenon lamp, can produce only 2 microwatts per square centimeter per angstrom at a distance of 50 centimeters from the excitation zone. Hence tunable visible lasers are at least 10^5 times brighter than conventional white-light sources. Moreover, this comparison does not include the large losses incurred in passing the white light through a monochromator in order to narrow the bandwidth.

In order for a molecule to be detectable by laser-induced fluorescence, there are three major requirements. The most obvious one is that the molecule fluoresces. Although this requirement is well satisfied in general for small molecules, particularly diatomic molecules, there are many polyatomic molecules known whose excited states undergo radiationless processes instead of fluorescing. Moreover, it is preferable that the quantum yield be 100 percent so that the conversion of fluorescence intensities to populations is not complicated by the variation of quantum yield with internal state.

The second requirement is that the band system be spectroscopically analyzed so that quantum members can be assigned and intensity factors, such as Franck-Condon factors and rotational line strengths, can be obtained. This requirement again favors the study of diatomic and small polyatomic molecules, of the sort discussed in Herzberg's classic texts (*16*).

The final requirement is that the molecular band system be accessible with available dye lasers. The wavelength range presently covered by pulsed dye lasers is from 3500 to 7300 angstroms, with the use of a series of about a dozen dye solutions, each of which lases over about 200 angstroms. This restricts present experiments to reaction products having low-lying excited electronic states, such as free radicals (for example, CN, CH, and NH_2) and metal compounds (for example, oxides, hydrides, and halides) (*31*). However, this restriction can be relaxed if nonlinear optics are used to generate ultraviolet laser light. By frequency-doubling or frequency-mixing the laser output with crystals, the wavelength limit has been extended to about 2000 angstroms (*32*). A large number of molecules have band systems within this spectral range. Nevertheless, such simple molecules as H_2 whose band systems lie in the vacuum ultraviolet cannot be detected at present with the use of tunable lasers. However, recent frequency-tripling techniques involving the use of gases are providing a means for breaching even this hitherto inaccessible region (*33*). Tunable laser operation has been achieved in the range from 1750 to 2000 angstroms.

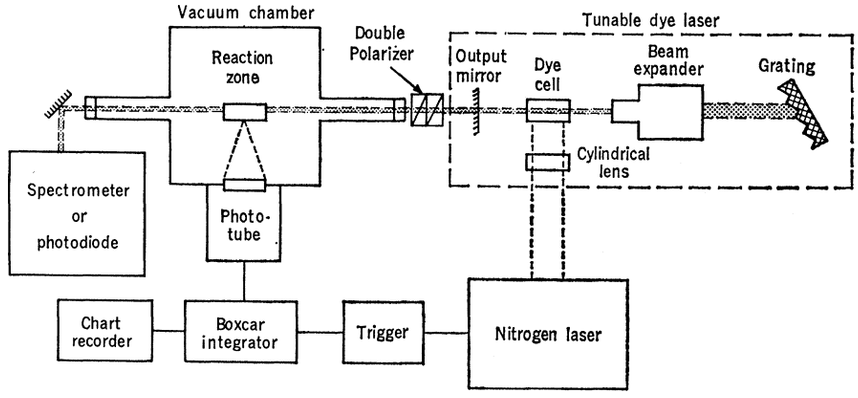

Fig. 4. Schematic of a laser-induced fluorescence apparatus. In this arrangement, the reaction zone is being directly irradiated. [Adapted from Cruse *et al.* (*36*)]

Laser-induced fluorescence is extremely sensitive and specific. Indeed, for the reaction $Ba + O_2 \rightarrow BaO + O$, it has been possible to detect in a particular (v,J) level a density as low as 5×10^4 BaO molecules per cubic centimeter, corresponding to an absorbance of only 10^{-8} (*34*). It is of interest to compare laser-induced fluorescence detection with mass spectrometric detection. The following simple argument shows that the detection efficiency is comparable *for those molecules irradiated*: When the laser is on, about 10 percent of those molecules that are in the excitation zone and in the correct internal state to absorb the laser light are excited. In fact, it is easy to obtain a larger percentage, but care must be taken to avoid optically pumping the sample (*35*) so that the conversion of the excitation spectrum to relative populations is straightforward. The excited molecules radiate into 4π steradians, and about 10 percent of the fluorescence may be conveniently collected by a photomultiplier. Finally, photomultipliers have typically a 10 percent quantum efficiency in the visible. Thus the overall efficiency is about 10^{-3}. The above estimate applies only to those molecules irradiated. In the $Ba + O_2$ experiment, in which a dye laser pumped with a pulsed nitrogen laser was used, the pulse repetition rate was 10 pulses per second and the pulse duration was $\sim 5 \times 10^{-9}$ second; hence the duty factor was extremely low. Ideally, the pulse rate of the laser should be equal to the rate of replenishment of molecules in the laser excitation zone ($\sim 5 \times 10^4$ pulses per second) so that all the molecules produced are exposed to the laser light. Since dye lasers with repetition rates of greater than 10^3 pulses per second and cw (continuous-wave) dye lasers are now available, it should be possible to increase the present detection sensitivity by several orders of magnitude and to approach that of a mass spectrometer.

Unlike the mass spectrometer, laser-induced fluorescence is not a universal detector, but it is highly specific and selective. The problems associated with mass spectrometry caused by interference from residual background gas and from contributions to the mass of interest through fragmentation are avoided. For instance, the OH radical would be easily detectable at $\sim$ 3000 angstroms, whereas mass analysis of OH is extremely difficult because of contributions to the OH^+ mass peak from the ubiquitous H_2O background. On the other hand, laser-induced fluorescence suffers from interference when several fluorescent species with overlapping absorption spectra are present. This may become a severe problem in the vacuum ultraviolet, where the residual background gas fluoresces. Like the mass spectrometer, laser-induced fluorescence measures a number density, whereas cross sections (rate constants) are defined in terms of the flux of molecules passing through a plane (density times velocity). Hence, for both detectors, some velocity information is necessary for the conversion of measured populations to cross sections.

Examples of Excitation Spectra

The first successful use of laser-induced fluorescence to measure internal state distributions of reaction products was reported in 1972 by Schultz, Cruse, and Zare (*34*), who presented preliminary data on the reaction $Ba + O_2 \rightarrow BaO + O$. Subsequently, the reactions of barium with the hydrogen halides were investigated by Cruse, Dagdigian, and Zare (*36*). Figure 4 shows a schematic drawing of the apparatus. A beam of barium atoms passes through a scattering chamber filled with gas at pressures of $\leq 10^{-3}$ torr ("beam-gas" arrangement). A tunable dye laser, patterned after the design of Hänsch (*30*), is used to excite the fluorescence. The dye laser is pumped with a pulsed nitrogen laser, and its optical cavity, formed by a partially reflecting output mirror and a diffraction grating, is arranged so that only a small wavelength range within the fluorescence spectrum of the dye has appreciable optical gain. The laser wavelength is scanned simply by rotating the grating with a motor drive. Because of the low duty factor of the laser, the signal from the photomultiplier is sampled with a boxcar integrator for a short time during and after the laser pulse. A boxcar integrator is an electronic instrument which averages a repetitive signal. The integrator is triggered by the same start pulse which triggers the laser. After a preset time delay the integrator begins to collect the signal, and this process continues for a preset time period (chosen here to be several radiative lifetimes). The fluorescence signal from many laser pulses is averaged, and the resultant d-c voltage drives a chart recorder. Figure 5 shows a typical excitation spectrum for $Ba + HCl \rightarrow BaCl + H$. The BaCl spectrum is not rotationally resolved since the rotational lines are very closely spaced with respect to the laser bandwidth (0.5 angstrom). However, relative vibrational populations $N_{v''}$ may be obtained from the vibrational band intensities $I_{v'v''}$ (*37*), which are equal to the height of the band heads (*38*) above the "background" due to the other rotational branches. Figure 6 shows the relative vibrational populations of the barium halide products deduced from these studies. The vibrational distributions are definitely not Boltzmann in character and, except for BaF, are smooth bell-shaped functions of vibrational energy showing population inversion. The average fraction of the total available reaction energy which appears as product vibration ranges from 12 percent for BaF to 36 percent for BaBr. Rough rotational distributions have been obtained for BaF and BaCl by convoluting calculated rotational line positions with the laser bandwidth. If various assumed rotational distributions are used, the average fraction of energy appearing as rotation is found to be about 15 percent. Hence, about 50 to 75 percent of the available reaction energy appears, on the average, as product translational energy. This is a surprisingly large percentage by comparison with previously studied reactions (*3*). The detailed vibrational distributions offer a severe test for present dynamical theories of chemical reactions.

Barium oxide is an example of a reaction product for which rotational

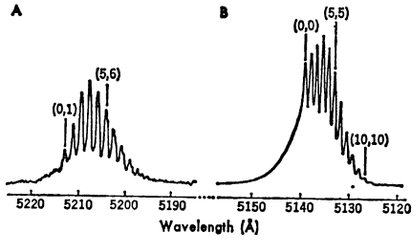

Fig. 5 (left). Excitation spectrum of BaCl for the $Ba + HCl \rightarrow BaCl + H$ reaction. The band heads of the $C\ ^2\Pi_{3/2} - X\ ^2\Sigma^+$ $\Delta v = v' - v'' = -1$ (A) and 0 (B) sequences are marked; the coordinate scale of (A) was six times more sensitive than that of (B). [Adapted from Cruse *et al.* (*36*)] Fig. 6 (right). Relative BaX vibrational populations for the reactions $Ba + HX \rightarrow BaX + H$. For each reaction, the populations have been normalized so that the population of the most probable level equals unity. [Adapted from Cruse *et al.* (*36*)]

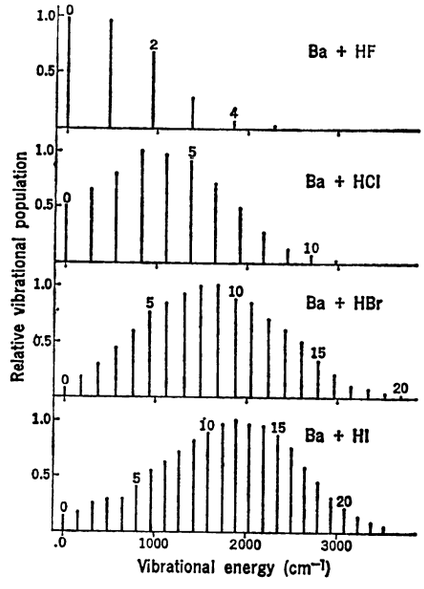

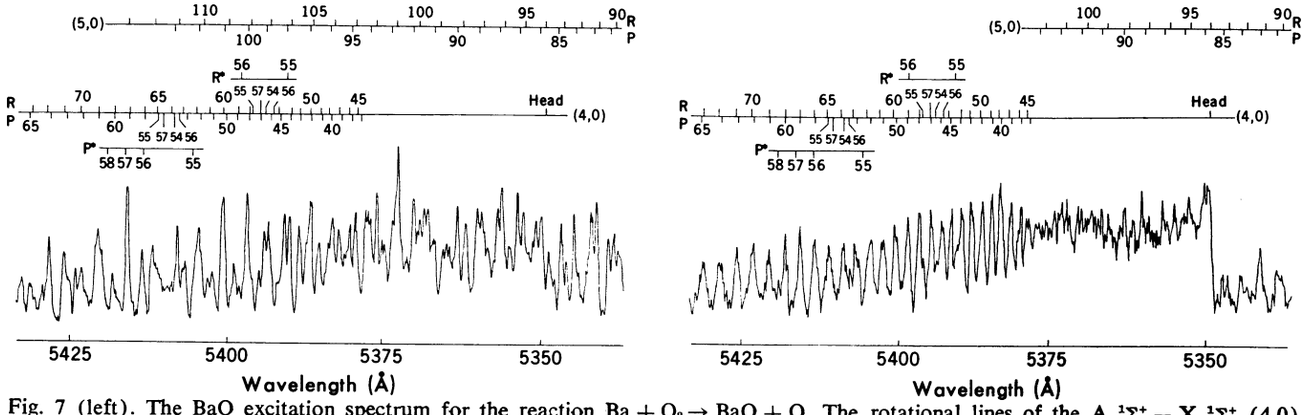

Fig. 7 (left). The BaO excitation spectrum for the reaction $Ba + O_2 \rightarrow BaO + O$. The rotational lines of the $A\ ^1\Sigma^+ - X\ ^1\Sigma^+$ (4,0) and (5,0) vibrational bands are marked; $R(J'')$ and $P(J'')$ denote lines for which $J' = J'' + 1$ and $J' = J'' - 1$, respectively. The effect of electronic perturbations in the A state is evident from the displacement of some lines and the appearance of new lines. Fig. 8 (right). The BaO excitation spectrum for the reaction $Ba + CO_2 \rightarrow BaO + CO$ for the same spectral region as that shown in Fig. 7.

information may be obtained since it is easy to rotationally resolve the BaO electronic spectrum. Figures 7 and 8 present BaO excitation spectra for the reactions $Ba + O_2 \rightarrow BaO + O$ and $Ba + CO_2 \rightarrow BaO + CO$, respectively. These spectra have been taken with an improved apparatus, for which collisional relaxation of BaO, which plagued early work (*34*), is insignificant (*39*). The difference in appearance and complexity of the BaO spectra between the two reactions is startling. For the $Ba + O_2$ reaction, all band heads are almost entirely missing. Since the band heads are formed for values of $J \sim 5$, this implies that the relative populations of low rotational states are very small. In addition, there are many more lines present, an indication that a larger number of vibrational levels are populated. Most of these high-J, and high-v lines cannot be identified since they have not been analyzed previously by high-resolution spectroscopy (*40*). On the other hand, all the lines in the $Ba + CO_2$ reaction can be assigned, and the band heads are clearly evident. The BaO rotational distributions for the $Ba + CO_2$ reaction can be characterized by a Boltzmann distribution with $T_{rot} = 2000° \pm 300°K$; the vibrational distribution also appears to be thermal in character, with a vibrational temperature T_{vib} slightly lower than T_{rot}. In contrast to the Ba + HX reactions, the $Ba + CO_2$ reaction appears to be characterized by the formation of a collision complex in which the reaction energy is partitioned equally among the available degrees of freedom. Because of the complexity of the $Ba + O_2$ reaction, only an approximate rotational distribution may be inferred. This is shown in Fig. 9, along with the $Ba + CO_2$ distribution for comparison. The striking feature of the $Ba + O_2$ reaction is that about one-third of the available reaction energy, on the average, appears as product BaO rotation.

The $Ba + O_2$ reaction has also been studied in a crossed-beam arrangement with mass spectrometric detection (*41, 42*). Although there has been disagreement on angular distribution measurements, the most recent experiments (*42*) show that the BaO products exhibit forward-backward symmetry in the CM system, an indication that the reaction proceeds through a long-lived collision complex. We have found that the experimental BaO rotational distribution shown in Fig. 9 is consistent with distributions calculated by statistical theories (*43*) appropriate for reactions proceeding via a persistent complex. Hence, the laser-induced fluorescence experiment and the molecular beam-scattering experiment can provide complementary views of the same reaction and give a virtually complete picture of the reaction dynamics.

Future Applications

Laser-induced fluorescence is a general detector and can be applied to a wide variety of gas-phase processes, even in high-pressure environments. In addition to reactive collisions, either neutral-neutral or ion-molecule, it may be used to advantage in the study of inelastic and elastic scattering processes. Laser-induced fluorescence can also provide information on the reaction energetics by identifying the highest internal product state populated in a given reaction. For example, a lower bound on the dissociation energy of AlO has been obtained (*44*) from a determination of the highest vibrational level of AlO populated in the reaction $Al + O_2 \rightarrow AlO + O$. Because chemical reactions can populate quantum states of molecules inaccessible under thermal conditions, laser-induced fluorescence also offers a powerful means of extending structural knowledge about the ground and excited states. For instance, the visible spectrum of the BaI molecule has been investigated with microwave discharges and flames (*45*). With these excitation sources, it has been possible to observe only the lowest vibrational levels ($0 \leq v \leq 8$) in the ground and excited states. Using laser-induced fluorescence, Cruse *et al.* have observed BaI vibrational levels up to $v = 25$ populated in the reaction $Ba + CH_3I$ and up to $v = 50$ in the reaction $Ba + CH_2I_2$ (*46*). This ability to observe highly excited levels of reaction products is also apparent from Fig. 7. Although often such information advances our knowledge of molecular structure, this wealth of data can be a hindrance to the derivation of dynamical information since the energy levels must be identified before a kinetic analysis can be carried out. As we have mentioned earlier, cw dye lasers offer the possibility of considerable gains in sensitivity; however, the use of pulsed lasers allows the direct measurement of radiative lifetimes in a simple manner free from most systematic errors, such as radiation trapping, quenching, and cascading, which have bedeviled measurements of radiative lifetimes in the past. Recently, the radiative lifetimes of about 40 electronic states of the alkaline earth monohalides have been determined to an accuracy of about 10 percent by this technique (*47*).

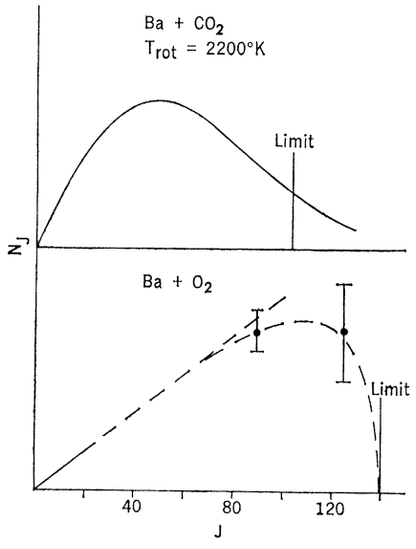

Fig. 9. Derived BaO rotational distributions in the $v'' = 0$ vibrational level for the $Ba + CO_2$ and $Ba + O_2$ reactions. The exoergicity limit is marked. The $Ba + CO_2$ distribution is drawn beyond the exoergicity limit because of the form of the assumed Boltzmann distribution.

As a molecular beam detector, laser-induced fluorescence has the virtue that the excitation zone can be positioned easily. For example, we can probe the reaction zone directly, which is not possible with other detectors. In almost all experiments carried out to date, the reaction zone and excitation zone have coincided. However, in the last few months we have succeeded in performing the first primitive angular distribution study (*48*). This work has shown that there is sufficient sensitivity so that it is possible to determine what internal states are scattered into what solid angle elements. This can be accomplished by positioning the excitation zone away from the reaction zone and by either rotating the reactant beams with respect to the excitation zone or vice versa. Such studies provide at least as much information as a product velocity analysis, if similar angular and velocity spreads are used in the reactant beams.

Laser-induced fluorescence can also be used to determine the orientation and alignment of the reaction products from studies of the degree of polarization of the fluorescence. In a reactive collision, the total angular momentum

is the sum of the initial internal angular momentum of the reactants (rotation), which is isotropic without special state preparation, and the initial orbital angular momentum $\mathbf{L}_i$ (see Fig. 3), which lies in a plane perpendicular to the initial relative velocity vector $\mathbf{v}_{rel}$. The measurement of the spatial distribution of the product rotational angular momentum $\mathbf{J}_f$ gives insight into the reaction dynamics since the transfer of the polarization of $\mathbf{L}_i$ to $\mathbf{J}_f$ depends sensitively on the details of the reactive collision (*49*). As mentioned earlier, Maltz *et al.* (*10*) have already observed the alignment of polar reaction products by electric deflection techniques. Although alignment studies have not been carried out yet on reactive systems by means of measurements of the degree of polarization of the fluorescence, the feasibility of this technique has been demonstrated by Sinha, Caldwell, and Zare (*50*), who determined the degree of alignment of alkali dimer molecules in a supersonic beam. Thus, there is every reason to believe that laser-induced fluorescence is particularly well suited to this task.

The velocity distribution of the products may be obtained by laser-induced fluorescence in several different ways. Since the translational energy is equal to the difference between the total reaction energy and the internal energy, the angular distribution as a function of internal state indirectly provides velocity information. On the other hand, velocity distributions may be measured directly by a time-of-flight method. Here one simply chops (interrupts) the beam and then fires the laser with a variable time delay. This method is applicable to the reactants and the products. Alternatively, velocity distributions can be determined by "Doppler spectroscopy," in which a very-narrow-bandwidth (50 megahertz) laser beam is tuned over the width of the Doppler-broadened spectral line. Although advances in laser technology have made this technique feasible, the interpretation of the resultant line shapes requires angular information. Moreover, if the product molecule has hyperfine structure, a knowledge of these splittings is necessary. Thus, it is possible to learn about the partitioning of the reaction energy into the various hyperfine levels of the products. Although this may be the ultimate in the detailed study of reactions, and even though we can imagine cases where such information does give insight (*51*), we suppose that this will not generally aid chemists in understanding reaction dynamics.

We foresee that laser-induced fluorescence, where applicable, will make it possible to specify product states as well as desired. Since the product translational and internal states observed result from an average over the reactant velocity and internal state distributions, we conclude that we are limited in the information obtainable unless we can better define the reactant states. Fortunately there has been much progress in this direction. We now have the ability to produce reactants in known translational states, for example, by supersonic beams (*52*), in known internal states, for example, by infrared laser excitation (*53*), and in known spatial orientations, for example, by electric deflection (*54*). With the use of laser-induced fluorescence, we should be able to observe how the energy of the reactants manifests itself in the various product states. Such experiments represent a giant step toward realizing the chemist's dream of determining microscopic reaction rates.

References and Notes

1. Excellent reviews of the field of molecular beams may be found in the following: N. F. Ramsey, *Molecular Beams* (Oxford Univ. Press, Oxford, England, 1956); R. G. J. Fraser, *Molecular Rays* (Cambridge Univ. Press, Cambridge, England, 1931); P. Kusch and V. W. Hughes, in *Handbuch der Physik*, S. Flügge, Ed. (Springer, Berlin, 1959), vol. 37, part 1, p. 1. A recent review of molecular beam electric resonance spectroscopy has been completed by J. C. Zorn and T. C. English, in *Advances in Atomic and Molecular Physics*, D. R. Bates and I. Estermann, Eds. (Academic Press, New York, 1973), vol. 9, p. 243.
2. For early reviews, see: S. Datz and E. H. Taylor, in *Recent Research in Molecular Beams*, I. Estermann, Ed. (Academic Press, New York, 1959), p. 157; W. L. Fite and S. Datz, *Annu. Rev. Phys. Chem.* **14**, 61 (1963); E. F. Greene, H. L. Moursund, J. Ross, *Adv. Chem. Phys.* **10**, 135 (1966); D. R. Herschbach, *ibid.*, p. 319; J. P. Toennies, in *Chemische Elementarprozesse*, H. Hartmann *et al.*, Eds. (Springer, Berlin, 1958), p. 157; J. P. Toennies, *Ber. Bunsenges Phys. Chem.* **72**, 927 (1968).
3. J. L. Kinsey, in *Medical and Technical Publishing Company International Review of Science, Physical Chemistry*, series 1, vol. 9, *Chemical Kinetics*, J. C. Polanyi, Ed. (University Park Press, Baltimore, 1972), p. 173. We highly recommend this review for a general discussion of recent molecular beam reactive scattering experiments. Present activity in this field can be judged, in part, by the Faraday Discussion on Molecular Beam Scattering [*Faraday Disc. Chem. Soc.* **55**, 1 (1973)].
4. See, for example, W. B. Miller, S. A. Safron, D. R. Herschbach, *Disc. Faraday Soc.* **44**, 108 (1967).
5. Descriptions of the construction and operation of velocity selectors include the following: R. C. Miller and P. Kusch, *Phys. Rev.* **99**, 1314 (1955); H. U. Hostettler and R. B. Bernstein, *Rev. Sci. Instrum.* **31**, 872 (1960); H. G. Bennewitz, thesis, Bonn University, Bonn, West Germany (1956).
6. T. P. Schafer, P. E. Siska, J. M. Parson, F. P. Tully, W. C. Wong, Y. T. Lee, *J. Chem. Phys.* **53**, 3385 (1970).
7. K. T. Gillen and R. B. Bernstein [*Chem. Phys. Lett.* **5**, 275 (1970)] have shown that vibrationally hot KI molecules can be detected on "desensitized" platinum-tungsten hot wires. The ionization efficiency is found to increase with the KI internal energy. In mass spectrometry the appearance potential and cross section are also known to vary with internal energy [see F. H. Field and J. L. Franklin, *Electron Impact Phenomena and the Properties of Gaseous Ions* (Academic Press, New York, 1957)]. Bolometer detectors also appear to be sensitive to the vibrational excitation of the products [see H. B. Alphin and G. A. Fisk, *Rev. Sci. Instrum.* **44**, 1786 (1973)].
8. R. R. Herm and D. R. Herschbach, *J. Chem. Phys.* **43**, 2139 (1965).
9. R. Grice, J. E. Mosch, S. A. Safron, J. P. Toennies, *ibid.* **53**, 3376 (1970).
10. C. Maltz, N. D. Weinstein, D. R. Herschbach, *Mol. Phys.* **24**, 133 (1972).
11. S. Freund, G. A. Fisk, D. R. Herschbach, W. Klemperer, *J. Chem. Phys.* **54**, 2510 (1971).
12. H. G. Bennewitz, R. Haerten, G. Müller, *Chem. Phys. Lett.* **12**, 335 (1971).
13. S. J. Riley and D. R. Herschbach, *J. Chem. Phys.* **58**, 27 (1973).
14. C. Maltz, thesis, Harvard University (1969).
15. R. P. Mariella, Jr., D. R. Herschbach, W. Klemperer, *J. Chem. Phys.* **58**, 3785 (1973).
16. G. Herzberg, *Molecular Spectra and Molecular Structure* (Van Nostrand, Princeton, N.J.; vol. 1, 1950; vol. 2, 1945; vol. 3, 1967).
17. See, for example, V. N. Kondratev, *Chemical Kinetics of Gas Reactions* (transl. by J. M. Crabtree and S. N. Carruthers) (Addison-Wesley, Reading, Mass., 1964).
18. N. C. Peterson, M. J. Kurylo, W. Braun, A. M. Bass, R. A. Keller, *J. Opt. Soc. Am.* **61**, 746 (1971); R. A. Keller, E. F. Zalewski, N. C. Peterson, *ibid.* **62**, 319 (1972); R. J. Thrash, H. Von Weyssenhoff, J. S. Shirk, *J. Chem. Phys.* **55**, 4659 (1971); G. H. Atkinson, A. H. Laufer, M. J. Kurylo, *ibid.* **59**, 350 (1973); T. W. Hänsch, A. L. Schawlow, P. E. Toschek, *Inst. Electr. Electron. Eng. J. Quantum Electron.* **QE-8**, 802 (1972).
19. O. R. Frisch, *Z. Phys.* **86**, 42 (1933); R. Schieder, H. Walther, L. Wöste, *Opt. Commun.* **5**, 337 (1972); J. L. Piqué and J. L. Vialle, *ibid.*, p. 402.
20. J. K. Cashion and J. C. Polanyi, *J. Chem. Phys.* **29**, 455 (1958); *ibid.* **30**, 1097 (1959).
21. D. H. Maylotte, J. C. Polanyi, K. B. Woodall, *ibid.* **57**, 1547 (1972); K. G. Anlauf, D. S. Harne, R. G. Macdonald, J. C. Polanyi, K. B. Woodall, *ibid.*, p. 1561; J. C. Polanyi and K. B. Woodall, *ibid.*, p. 1574; A. M. G. Ding, L. J. Kirsch, D. S. Perry, J. C. Polanyi, J. L. Schreiber, *Faraday Disc. Chem. Soc.* **55**, 252 (1973), and references therein.
22. N. Jonathan, C. M. Melliar-Smith, D. H. Slater, *Mol. Phys.* **20**, 93 (1971); N. Jonathan, C. M. Melliar-Smith, S. Okuda, D. H. Slater, D. Timlin, *ibid.* **22**, 561 (1971).
23. J. D. McDonald, *Faraday Disc. Chem. Soc.* **55**, 376 (1973); J. G. Moehlmann and J. D. McDonald, *J. Chem. Phys.* **59**, 6683 (1973).
24. For example, see: J. H. Parker and G. C. Pimentel, *J. Chem. Phys.* **51**, 91 (1969); G. Hancock, C. Morley, I. W. M. Smith, *Chem. Phys. Lett.* **12**, 193 (1971); M. J. Berry, *J. Chem. Phys.* **59**, 6229 (1973); M. J. Molina and G. C. Pimentel, *Inst. Electr. Electron. Eng. J. Quantum Electron.* **QE-9**, 64 (1973).
25. C. Ottinger and R. N. Zare, *Chem. Phys. Lett.* **5**, 243 (1970).
26. C. D. Jonah, R. N. Zare, C. Ottinger, *J. Chem. Phys.* **56**, 263 (1972).
27. J. L. Gole and R. N. Zare, *ibid.* **57**, 5331 (1972).
28. R. C. Oldenborg, J. L. Gole, R. N. Zare, *ibid.* **60**, 4032 (1974); W. S. Struve, J. R. Krenos, D. L. McFadden, D. R. Herschbach, in preparation.
29. P. P. Sorokin and H. R. Lankard, *IBM J. Res. Dev.* **10**, 162 (1966).
30. T. W. Hänsch, *Appl. Opt.* **11**, 895 (1972).
31. See: W. M. Jackson, *J. Chem. Phys.* **59**, 960 (1973); J. A. Cruse and R. N. Zare, *ibid.* **60**, 1182 (1974).
32. Examples of frequency-doubled tunable lasers include the following: B. G. Huth, G. I. Farmer, L. M. Taylor, M. R. Kagan, *Spectrosc. Lett.* **1**, 425 (1968); D. A. Jennings and A. J. Varga, *J. Appl. Phys.* **42**, 5171 (1971); F. B. Dunning, E. D. Stokes, R. F. Stebbings, *Opt. Commun.* **6**, 63 (1972). For more recent work, see A. L. Robinson, *Science* **184**, 1165 (1974).
33. S. E. Harris and R. B. Miles, *Appl. Phys. Lett.* **19**, 385 (1971); J. F. Young, G. C. Bjorklund, A. H. Kung, R. B. Miles, S. E. Harris, *Phys. Rev. Lett.* **27**, 1551 (1971); R.

B. Miles and S. E. Harris, *Inst. Electr. Electron. Eng. J. Quantum Electron.* **QE-9**, 470 (1973); R. T. Hodgson, P. P. Sorokin, J. J. Wynne, *Phys. Rev. Lett.* **32**, 343 (1974).
34. A. Schultz, H. W. Cruse, R. N. Zare, *J. Chem. Phys.* **57**, 1354 (1972).
35. R. E. Drullinger and R. N. Zare, *ibid.* **51**, 5532 (1969); *ibid.* **59**, 4225 (1973).
36. H. W. Cruse, P. J. Dagdigian, R. N. Zare, *Faraday Disc. Chem. Soc.* **55**, 277 (1973).
37. Vibrational bands are designated by (v',v''), where v' and v'' refer to the vibrational quantum numbers of the upper and lower electronic states, respectively.
38. Band heads arise because the frequencies of rotational lines in a given vibrational band do not vary monotonically as a function of rotational level. There is a turning point in frequency, where the rotational lines pile up and overlap to produce a maximum in intensity. On one side of the head the intensity falls suddenly to zero, whereas on the other the falloff is much more gradual.
39. P. J. Dagdigian, H. W. Cruse, A. Schultz, R. N. Zare, *J. Chem. Phys.*, in press.
40. A. Lagerqvist, E. Lind, R. F. Barrow, *Proc. Phys. Soc. Lond. Sect. A* **63**, 1132 (1950).
41. C. B. Cosmovici and K. W. Michel, *Chem. Phys. Lett.* **11**, 245 (1971); J. Fricke, B. Kim, W. L. Fite, in *Proceedings of the 7th International Conference on the Physics of Electronic and Molecular Collisions, Abstracts of Papers*, T. R. Govers and F. J. de Heer, Eds. (North-Holland, Amsterdam, 1971), p. 37.
42. H. J. Loesch and D. R. Herschbach, in preparation.
43. S. A. Safron, N. D. Weinstein, D. R. Herschbach, J. C. Tully, *Chem. Phys. Lett.* **12**, 564 (1972); P. Pechukas, J. C. Light, C. Rankin, *J. Chem. Phys.* **44**, 794 (1966), and references therein.
44. P. J. Dagdigian, H. W. Cruse, R. N. Zare, preliminary results [reported by R. N. Zare, *Ber. Bunsenges. Phys. Chem.* **78**, 153 (1974)].
45. P. Mesnage, *Ann. Phys. (Paris)* **12** (No. 11), 5 (1939); M. N. Patel and N. R. Shah, *Ind. J. Pure Appl. Phys.* **8**, 681 (1970); B. R. K. Reddy and P. T. Rao, *J. Phys. B* **3**, 1008 (1970).
46. H. W. Cruse, P. J. Dagdigian, R. N. Zare, in preparation.
47. P. J. Dagdigian, H. W. Cruse, R. N. Zare, *J. Chem. Phys.* **60**, 2330 (1974).
48. P. J. Dagdigian and R. N. Zare, *ibid.*, in press.
49. D. R. Herschbach, *Disc. Faraday Soc.* **33**, 149 (1962); *ibid.*, p. 277; *ibid.*, p. 278; *ibid.*, p. 281.
50. M. P. Sinha, C. D. Caldwell, R. N. Zare, *J. Chem. Phys.*, in press.
51. For example, populations of hyperfine levels produced by chemical reactions may be of importance in explaining maser action in the interstellar medium.
52. M. E. Gersh and R. B. Bernstein, *J. Chem. Phys.* **55**, 4661 (1971); *ibid.* **56**, 6131 (1972); S. B. Jaffe and J. B. Anderson, *ibid.* **49**, 2859 (1968); *ibid.* **51**, 1059 (1969); J. G. Pruett, F. R. Grabiner, P. R. Brooks, *ibid.* **60**, 3335 (1974).
53. T. J. Odiorne, P. R. Brooks, J. V. V. Kasper, *ibid.* **55**, 1980 (1971).
54. P. R. Brooks and E. M. Jones, *ibid.* **45**, 3449 (1966); R. J. Beuhler, Jr., R. B. Bernstein, K. H. Kramer, *J. Am. Chem. Soc.* **88**, 5331 (1966); R. J. Beuhler, Jr., and R. B. Bernstein, *Chem. Phys. Lett.* **2**, 166 (1968); *ibid.* **3**, 118 (1969); *J. Chem. Phys.* **51**, 5305 (1969); P. R. Brooks, *Faraday Disc. Chem. Soc.* **55**, 299 (1973); *ibid.*, p. 318.
55. J. D. McDonald, P. R. LeBreton, Y. T. Lee, D. R. Herschbach, *J. Chem. Phys.* **56**, 769 (1972).
56. This work was supported by the Air Force Office of Scientific Research under grants AFOSR-72-2275, AFOSR-73-2551, and AFOSR-73-2551A, by the Army Research Office (Durham) under grant DA-ARO-D-31-124-73-G147, and by the National Science Foundation under grant NSF-GP-31336.

Thermoregulation in Endothermic Insects

Body temperature is closely attuned to activity and energy supplies.

Bernd Heinrich

In insects, as in other animals, body temperature is one parameter affecting the rate of energy expenditure, the rate at which food can be located and harvested, and the facility with which predators can be avoided. A "poikilothermic" caterpillar (*1, 2*) may be restricted for weeks to one plant where it ingests large quantities of leaf tissue. The small percentage of nutrients extracted from the large bulk of this foodstuff (*3*) is channeled primarily into body tissues. A "heterothermic" (*4*) moth, on the other hand, is often highly mobile while feeding from scattered flowers. It utilizes high-energy fuels (*5*) which permit intense metabolic rates that cause endothermy (heat production at rates sufficient to increase body temperature).

Endothermy, as such, has long been known to exist in insects (*6*). In 1837, 6 years after thermocouples were first used to measure the body temperature of insects (*7*), Newport (*8*) reported that sphinx moths and bumblebees may elevate their thoracic temperature above ambient temperature by muscular activity. Preflight warm-up was described by Dotterweich in 1928 (*9*), and in 1965 Heath and Adams (*10*) reported that the sphinx moth *Celerio lineata* stabilizes its thoracic temperature during flight over a range of ambient temperatures. It has only recently been demonstrated that some insects regulate their body temperature by physiological means. The regulation of body temperature by behavioral means such as basking, on the other hand, is a well-established phenomenon. It has been described in the desert locust *Schistocerca gregaria* (*11*), in butterflies (*12*), beetles (*13, 14*), cicadas (*15, 16*), and arctic flies (*17*).

Various aspects of thermoregulation in insects have been reviewed (*18, 19*), but at the time these articles were written, little was known about the mechanisms involved. I will here examine recent developments and comparative aspects of insect physiology relating to thermoregulation in the contexts of energetics and ecology.

Muscle Activity and Endothermy

In insects, essentially all endothermic increases of body temperature above ambient temperature are the result of heat produced by the active flight muscles. These muscles are, metabolically, the most active tissues known (*20, 21*). The mechanical efficiency of the flight mechanism of both insects and birds is approximately 10 to 20 percent (*22*); more than 80 percent of the energy expended during flight is necessarily degraded to heat. Flight activity and endothermy are thus invariably linked, at least in the larger insects (*20, 23*), and endothermy in flight is in large part an obligatory phenomenon.

Body temperature during flight and stridulation. A high muscle temperature is not only a consequence of muscle activity. It is also a prerequisite for flight. In order to lift a load in free flight, or to fly at a certain speed, the insect must exert a specific force per wingbeat and maintain a minimum wingbeat frequency. This requires that the contractions of the upstroke and downstroke muscle be sufficiently rapid

The author is assistant professor of entomology in the Department of Entomological Sciences, University of California, Berkeley 94720.